Mid-infrared difference–frequency generation in periodically poled KTiOAsO$_4$ and application to gas sensing

K. Fradkin-Kashi, A. Arie, P. Urenski, and G. Rosenman

Department of Electrical Engineering—Physical Electronics, Faculty of Engineering, Tel Aviv University, Tel Aviv 69978, Israel

Tunable mid-infrared radiation (3.45−3.75 μm) with a power level of 0.14 μW is generated by quasi-phase-matched difference-frequency mixing of a Nd:YAG laser and a tunable-diode laser (near 1.5 μm) in multigrating periodically poled KTiOAsO$_4$. The wavelength and temperature bandwidths are $\approx$65 nm cm and $\approx$62 °C cm, respectively. The temperature-tuning slope of the phase-matched idler wavelength, -0.94 nm/°C, is almost twice that of periodically poled KTiOPO$_4$. We use the measurements to derive a mid-infrared-corrected Sellmeier equation for the Z axis of KTiOAsO$_4$. The generated mid-infrared radiation is applied to sensitive high-resolution spectroscopy of the ν_3 band of methane. © 2000 Optical Society of America

OCIS codes: 190.4360, 190.4400, 300.6340.

Difference-frequency mixing in nonlinear materials is a powerful method for producing mid-infrared (mid-IR) coherent radiation sources by use of compact and efficient lasers, which now exist principally in the near-IR region. The wide and easily controlled frequency tunability as well as the high spectral resolution of available near-IR lasers can be transferred to the mid-IR region by difference-frequency generation (DFG). Unlike optical parametric oscillators (OPO's), DFG interactions produce an idler whose wavelength is directly determined by the wavelengths of the pump and signal sources, thus making the DFG processes much more attractive for spectroscopic applications.

Quasi-phase matching between the interacting waves can be obtained by periodic modulation of the nonlinear coefficient. This permits noncritical phase matching of any desired interaction within the transparency range of the crystal with relatively high efficiency. In ferroelectric materials, quasi-phase matching can be achieved by application of a strong electric field through periodically patterned electrodes. This poling technique was successfully applied to several crystals, including LiNbO$_3$,[1] KTiOPO$_4$ (KTP),[2,3] RbTiOAsO$_4$,[4] and recently also to KTiOAsO$_4$ (KTA) crystals,[5] but most of the quasi-phase-matched DFG experiments were performed in periodically poled (PP) LiNbO$_3$.[6,7] Lately we have explored the optical properties of PP KTP in the mid-IR range by DFG.[8] KTP has a much higher damage threshold than LiNbO$_3$ but unfortunately also exhibits significant absorption at $\approx$3.3 μm and has a cutoff wavelength of $\approx$4 μm.

Another member of the KTP family is KTA, which enjoys both a high damage threshold, comparable with or slightly higher than that of KTP,[9] and has a higher cutoff wavelength of $\approx$4.85 μm. In addition, the significant absorption at $\approx$3.3 μm that exists in KTP is absent from KTA crystals.[10] Until now, PP KTiOAsO$_4$ (PP-KTA) crystals were used only for OPO interactions.[5] In this Letter we report, for the first time to the best of our knowledge, DFG of mid-IR coherent radiation with a PP-KTA crystal. Furthermore, this measurement enables us to characterize the optical and nonlinear properties of PP-KTA in the mid-IR range.

The DFG experimental setup is shown in Fig. 1. It employs two compact laser sources: a diode-pumped Nd:YAG laser at 1064.4 nm (Lightwave Electronics, Model 122) and an external-cavity tunable-diode laser near 1.5 μm (New-Focus, Model 6328-H) with a tuning range of 100 nm. The beams of the pump and signal lasers are combined collinearly with a dichroic beam splitter and focused into an uncoated 1-cm-long multigrating PP-KTA crystal (grating periods: 38.6, 38.9, and 39.2 μm). The KTA crystal (grown by Crystal Associates) was poled by the low-temperature electric-field poling technique.[5] By applying an electric field of 5.5 kV/mm at a temperature of 145 K, we obtained a homogeneous domain grating with an area of 8 mm × 10 mm with an approximately 50% duty cycle. We monitored the domain-reversal process by the pyroelectric method.

Our configuration uses the largest nonlinear coefficient in KTA, $d_{33} = 16.2$ pm/V.[10] Mid-IR radiation at 3.45−3.75 μm is generated in the PP-KTA crystal and focused onto a 1-mm-diameter liquid-nitrogen-cooled HgCdTe (MCT) detector (Fermionics, Model PV-6-1). The detector, used in the photovoltaic mode, exhibits a noise-equivalent power of $\approx$1 pW/$\sqrt{\text{Hz}}$. A tilted uncoated germanium window, placed in front of the detector, blocks the pump and the signal beams. The signal beam is chopped at a rate of 1.5 kHz, and the idler signal is detected with a lock-in-amplifier. The wavelengths of the pump and the signal lasers are measured with a Burleigh WA-20 wavemeter.

With 117.2 mW of Nd:YAG power at 1064.4 nm and 17.4 mW of diode power at 1519.6 nm incident upon
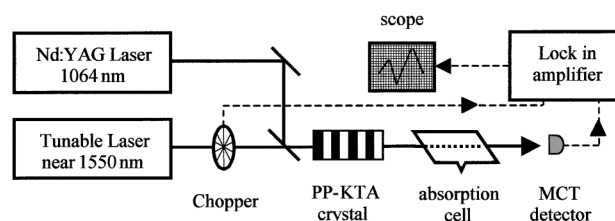

Fig. 1. Experimental setup for DFG of mid-IR radiation in a PP-KTA crystal.

the uncoated mixing crystal with period 39.2 μm, a maximum idler power of 0.103 μW is measured at the detector. When the transmission of all uncoated components in the setup is taken into account, this measured IR power indicates a normalized internal conversion efficiency of 0.0091%/(W cm).

The theoretical expression for DFG efficiency for the case of two Gaussian beams with a joint waist location at the middle of the crystal is[11] (in MKS units)

$$\eta = \frac{P_i}{P_p P_s l} = \frac{4\omega_i^2 k_s d_{\text{eff}}^2 h(\xi, \mu, \Delta k)}{\pi n_p n_s n_i \epsilon_0 c^3 (1 + \mu)}, \qquad (1)$$

where ω_i is the idler angular frequency; k_s is the signal wave vector; d_{eff} is the effective nonlinear coefficient; n_p, n_s, and n_i are the refractive indices of pump, signal, and idler wavelengths, respectively; ϵ_0 and c are the permittivity and the speed of light in free space, respectively; μ is the ratio between the signal and the pump wave vectors; ξ is the ratio between the crystal length and the confocal parameter; Δk is the wave-vector mismatch; and $h(\xi, \mu, \Delta k)$ is the focusing function, which assumes equal confocal parameters for the pump and the signal beams. However, our beams have different confocal parameters as well as slightly shifted waist positions. For DFG interactions with unequal confocal parameters, the focusing function is given in Ref. 12; nevertheless it still assumes a joint waist position in the middle of the crystal. Because of a slight difference in definition between Refs. 11 and 12, one has to multiply the focusing function of Ref. 12 by a factor of 2 before substituting it into Eq. (1). In our experiment both beams are slightly elliptic, with average beam radii of $\omega_{0p} \approx 19$ μm and $\omega_{0s} \approx 58$ μm, and $\mu \approx 0.7$. Assuming that $d_{\text{eff}} = (2/\pi)d_{33} \approx 9$ pm/V (taking into account Miller's delta), the theoretical conversion efficiency should be 0.024%/(W cm). The difference between the measured and the calculated efficiencies is due mostly to the nonideal spatial overlap between the pump and the signal beams that have different waist positions, a significant effect that is not taken into account by the focusing function of Ref. 12.

The DFG power as a function of the generated idler wavelength at room temperature (25 °C) is shown in Fig. 2 for three gratings, with periods 38.6, 38.9, and 39.2 μm. The FWHM for the idler wavelengths is $\approx$65 nm. The asymmetry of the detuning curve is a result of the tightly focused Gaussian beams.[12] Unlike in the case of plane-wave interactions, the highest efficiency is obtained at a nonzero wave-vector mismatch. In our experiment it was typically $\approx$300 m^{-1}. We also measured the DFG power as a function of the crystal temperature. For the 39.2-μm grating period, and with signal wavelengths of 1524.3 and 1528.3 nm, the peak efficiency was measured at temperatures of $\approx$52 °C and $\approx$72 °C, respectively. The derived tuning slope for the idler wavelength, -0.94 nm/°C, is considerably higher than that measured for PP KTP, -0.5 nm/°C,[8] but is still lower than the calculated slope for PP LiNbO$_3$,[13] -1.5 nm/°C. The large temperature-tuning slope of PP-KTA can be advantageous for fabricating other tunable devices, e.g., temperature-tuned OPO's.[14] We

have also measured a conveniently wide temperature FWHM of $\approx$62 °C, nearly twice that of PP LiNbO$_3$.[13]

Although a number of Sellmeier equations for KTA appear in the literature, Fenimore *et al.*[15] give the closest prediction of the phase-matched idler wavelengths. With a pump wavelength of 1064.446 nm at room temperature, idler wavelengths of 3.736, 3.643, and 3.551 μm were generated with periods of 38.6, 38.9, and 39.2 μm, respectively. However, there is still a relatively large deviation ($\approx$3%) from the experimental results. We used our measurements to calculate Sellmeier coefficients with improved accuracy in the mid-IR range. The general form of the refractive index in the Z direction of KTA is

$$n_z^2 = A + \frac{B}{1 - (C/\lambda)^2} + \frac{D}{1 - (E/\lambda)^2} - F\lambda^2. \qquad (2)$$

Initially we attempted to fit our experimental data in the 1.48–3.75-μm range, as well as measurements of Fenimore *et al.*[15] in the 0.8–1.3-μm range, using a reduced form of Eq. (2) with a single pole in the UV range, as was used in the research reported in Ref. 15. The best fit that we achieved still had a deviation of as much as 0.6% in predicting the phase-matched idler wavelength. Therefore we added a second pole in the mid-IR region and in this way improved the accuracy of the fit to 0.2%. The parameters of this fit are as follows: $A = 1.214331$, $B = 2.225328$, $C = 0.178542$, $D = 0.310017$, $E = 8.989998$, and $F = 0.009381$, where λ is given in micrometers. We used this new Sellmeier equation to calculate the expected phase-matching curves at room temperature. These curves appear in Fig. 2 together with the measured data, and it can be seen that, in addition to the equation's correctly predicting the location of the central peak, the calculated wavelength of the first sideband nearly coincides with the measured one. The nonzero wave-vector mismatch for the tightly focused Gaussian beams[12] was taken into account in the calculation of the Sellmeier coefficients. The calculated
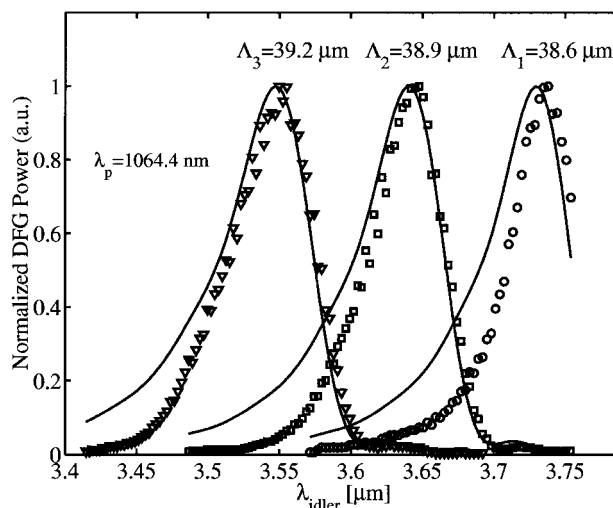

Fig. 2. Normalized DFG power as a function of the generated wavelength, as measured with a multigrating PP-KTA crystal (points: 38.6 μm, circles; 38.9 μm, squares; 39.2 μm, triangles). Solid curves were calculated with Eq. (2).
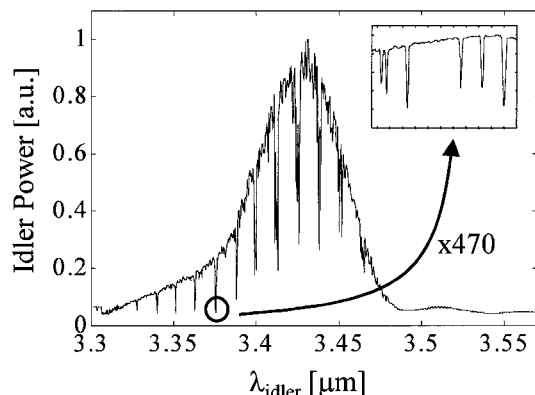
Fig. 3. ν_3 band of methane (P branch) measured at 77 Torr by DFG interaction in a PP-KTA crystal. Inset, high-resolution scan of $P(6)$ at 1 Torr.

bandwidth of ≈ 70 nm cm is in good agreement with the measured bandwidth of ≈ 65 nm, thus indicating that the PP length is approximately the entire 1-cm physical length of the crystal. It is also encouraging to note that Eq. (2), with the fit parameters stated above, accurately predicts the generated wavelengths of a Nd:YAG-pumped OPO in PP-KTA.[5] Furthermore, it is also in excellent agreement with a measurement given in Table 1 of Ref. 9 (n_y is taken from Ref. 15).

We used our mid-IR source to measure the absorption spectrum of methane near the ν_3 band at 3.3 μm, using a 10-cm-long gas cell. The wide tunability of the source enabled us to cover the entire P branch (3.3–3.48 μm) by using the 39.2-μm grating and with the crystal heated to a temperature of 140 °C. We measured the P branch under various methane pressures (see Fig. 3). The residual envelope that exists even when one is measuring in vacuum is due to the inherent phase-matching efficiency curve of the nonlinear interaction. The generated coherent source has a narrow linewidth, of the order of ≈ 1 MHz, which permits high-spectral-resolution measurements to be performed. For example, the splitting of the $P(6)$ line into six hyperfine components is clearly seen in the inset of Fig. 3.

We also performed measurements of gas concentration when the gas was mixed with room air. The minimum detectable concentration $C_{\min}$ is given by

$$C_{\min} = \frac{\pi \Delta T_{\min} k_{\mathrm{ap}} P_{\mathrm{air}}}{LS},\qquad(3)$$

where $\Delta T_{\min}$ is the minimum detectable transmission, k_{ap} is the half-width air-broadening coefficient, P_{air} is the air pressure, L is the absorption path length, and S is the line strength. We have assumed here that the main broadening mechanism is air-pressure broadening. We find the fractional concentration of methane by dividing $C_{\min}$ by the air concentration. For the $P(6)$ transition, typical values of S and k_{ap} are $\approx 10^{-19}$ cm/molecule and ≈ 0.06 cm^{-1}/atm, respectively. Because neither the optical elements nor the crystal was antireflection coated, the measurements exhibited significant etalon effects; thus $\Delta T_{\min} \approx 0.01$. As the absorption cell length is 10 cm, the minimum detectable concentration at room temperature is ≈ 75

parts in 10^6. One could achieve a significant improvement in sensitivity by increasing the absorption path length. For example, with a multipass cell of ≈ 30 m, the minimum detectable concentration would reach ≈ 255 parts in 10^9. Additional improvement may be attained by antireflection coating of the optical elements and the crystal, hence reducing the noise level to the detector limit.

In conclusion, we have demonstrated a PP-KTA-based widely tunable continuous-wave single-frequency DFG source operating in the mid-IR region, where many of the interesting molecules exhibit their strongest absorption lines. We have shown that this compact and robust source is suitable for high-resolution spectroscopy. The potential sensitivity for measuring methane concentration is in the sub-parts-in-10^6 range. The measured conversion efficiency of 0.0091%/(W cm) is comparable with results obtained with other crystals in this wavelength range. We have calculated a dispersion equation for KTA with improved accuracy in the mid-IR range. The temperature and wavelength tuning bandwidths were measured, and the temperature-tuning slope was found to be much larger than that of PP KTP. The wide transparency range, large nonlinearity, high damage threshold, and surprisingly high temperature-tuning coefficient make PP-KTA a most attractive material for nonlinear devices.

References

1. M. Yamada, N. Nada, M. Saitoh, and K. Watanabe, Appl. Phys. Lett. **62,** 435 (1993).
2. Q. Chen and W. P. Risk, Electron. Lett. **30,** 1516 (1994).
3. G. Rosenman, A. Skliar, D. Eger, M. Oron, and M. Katz, Appl. Phys. Lett. **73,** 3650 (1998).
4. H. Karlsson, F. Laurell, P. Henriksson, and G. Arvidsson, Electron. Lett. **32,** 556 (1996).
5. G. R. Rosenman, A. Skliar, Y. Findling, P. Urenski, A. Englander, P. A. Thomas, and Z. W. Hu, J. Phys. D **32,** L49 (1999).
6. S. Sanders, R. J. Lang, L. E. Myers, M. M. Fejer, and R. L. Byer, Electron. Lett. **32,** 218 (1996).
7. K. P. Petrov, R. F. Curl, and F. K. Tittel, Appl. Phys. B **66,** 531 (1998).
8. K. Fradkin, A. Arie, A. Skliar, and G. Rosenman, Appl. Phys. Lett. **74,** 914 (1999).
9. W. R. Bosenberg, L. K. Cheng, and J. D. Bierlein, Appl. Phys. Lett. **65,** 2765 (1994).
10. L. K. Cheng and J. D. Bierlein, Ferroelectrics **142,** 209 (1993).
11. T. B. Chu and M. Broyer, J. Phys. (Paris) **46,** 523 (1985).
12. S. Guha, F.-J. Wu, and J. Falk, IEEE J. Quantum Electron. **QE-18,** 907 (1982).
13. D. H. Jundt, Opt. Lett. **22,** 1553 (1997).
14. A. Garashi, A. Arie, A. Skliar, and G. Rosenman, Opt. Lett. **23,** 1739 (1998).
15. D. L. Fenimore, K. L. Schepler, U. B. Ramabadran, and S. R. McPherson, J. Opt. Soc. Am. B **12,** 794 (1995).